PHOTOELECTRIC AND PHOTOCAPACITANCE CHARACTERISTICS OF Au/PYRENE/n-Si MIS STRUCTURES

I. ARSEL*, M. TURMUŞ, O. PAKMA, C. ÖZAYDIN, Ö. GÜLLÜ
Department of Physics, Faculty of Sciences and Arts, Batman University, Batman, Turkey

This paper presents in-depth analysis of the current-voltage (*I-V*) and capacitance-voltage (*C-V*) characteristics of identically prepared Au/Pyrene($C_{16}H_{10}$)/*n*-Si hybrid organic-on-inorganic semiconductor photovoltaic cells (total 43 diodes). The barrier heights, ideality factors and reverse bias saturation currents of all devices were extracted from the electrical characteristics. The mean barrier height, mean ideality factor and mean saturation current from *I-V* measurements were calculated as 0.79 ± 0.01 eV, 1.40 ± 0.08 and (1.01 ± 0.46)x10^{-8} A, respectively. Also, the photoelectric (I-V) and photocapacitance (C-V and conductance (G)-voltage (V)) characteristics of the Au/Pyrene/n-Si device under 100 mW/cm^2 light illumination were investigated. It has been seen that the light illumination increases strongly the current, capacitance and conductance values of the device due to electron-hole charge pair generation. The C-V and G-V characteristics under illumination have shown a non-monotonic dependence of capacitance on frequency giving rise to a peak. This is attributed to the existence of electrically active traps. The open circuit voltage and short circuit current of the Au/Pyrene/n-Si device were extracted as 80 mV and 30 µA, respectively.

(Received March 13, 2017; Accepted May 26, 2017)

Keywords: Schottky barrier; ideality factor; Organic-Inorganic contact; Hybrid photovoltaic cell; Pyrene

1. Introduction

The interfaces of Metal/Semiconductor (MS) diode structures have implicitly been assumed to be laterally uniform and it has been seen that the junctions were characterized by their barrier heights (BHs) and ideality factors [1,2]. Mott defined the barrier height of MS contact as the difference of the semiconductor electron affinity and the related metal work function[3]. The ideality factor (*n*) can be found from its forward current–voltage (I-V) characteristics [3-4]. Barrier height and ideality factor are the fundamental parameters of Schottky structures [5]. Although they have been studied for over 50 years, it is only during the last decade that inhomogeneity of the Schottky device interface has been considered [3,6]. In the early 1990's, Tung [5,8-10], Werner et al.[7] and Biber et al.[11] mentioned that the BH is likely to be a function of the interface atomic structure, and the atomic inhomogeneities at the MS interface which are caused by facets, defects, grain boundaries and mixture of different phases. However, Tung et al. [5,8-10], and Sullivan et al. [8], and Rau et al. [12] already pointed out that inhomogeneities may play an important role and have to be taken into consideration in the evaluation of experimental current-voltage (*I-V)* measurements. The application of standard procedures to these characteristics gives effective BHs and ideality factors only. Both parameters change from diode-to-diode even if they are identically prepared. Recently, Tung and co-workers [5,8-10] studied theoretically and Mönch and co-workers [1,2] showed experimentally, that a correlation exists between effective BHs and ideality factors, which may be approximated by a linear relationship [1,2]. This result has been attributed to the barrier inhomogeneities [1,2,13-15]. Some authors have also reported experimental evidence that nanometer-sized lateral variations in BHs exist [16-18]. It was only during the last decade that by considering the inhomogeneities of the MS interface these devices have attracted much

* Corresponding author: ismail.arsel@batman.edu.tr

attention and progressed to play a crucial role in constructing some useful devices in electronic technology as well as being used for technical deficiencies such as surface processing, clean room, vacuum preparation and deposition techniques to produce proper contacts [19].

Metal/interlayer/Semiconductor (MIS) devices formed by organic thin layers grown on inorganic semiconductor substrates have extensively been investigated by many researchers for their potential use in the electronic and optoelectronic technologies so far. For example, many devices using the polymeric [20-25] and nonpolymeric organic materials [26-33] have been fabricated by including light emitting diodes and Schottky-type devices like an MIS structures and their electrical and photoelectrical properties have been investigated for more than three decades. Pyrene with molecular formula $C_{16}H_{10}$ used in the present work is a typical conjugated organic compound. The molecular structure of Pyrene is shown in Fig. 1. Pyrene is well known due to intense fluorescence with long life time and strong excimer emission and widely used as phohtophysical probe [34-37].

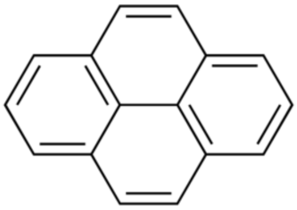

Fig 1. Molecular structure of Pyrene organic compound.

Recently, some researchers in the literature have reported similar studies by using an oxide interlayer in metal/interlayer/semiconductor structures [38,39]. For example Altindal and co-workers [39] have recently investigated the I-V and capacitance-voltage (C-V) characteristics of identically prepared Al/oxide/p-Si MIS structures (total 33 diodes). They [39] have shown that even though they were identically prepared, the Schottky barrier diodes reveal different BHs, ideality factors, series resistance and density of interface states. They [39] have found that there was a linear relationship between the experimental effective SBHs and ideality factors of Al/oxide/p-Si Schottky diodes. The experimental BH distributions obtained from the I–V and C^{-2}–V characteristics have been fitted by a Gaussian function, and their mean values have been calculated to be 0.708 and 0.810 eV, respectively [39].

In this work, we identically prepared the Au/Pyrene/n-Si Schottky photovoltaic structures on the same inorganic n-type Si semiconductor wafer and then, calculated the electrical parameters of each device by using the *I-V* and *C-V* measurements. The obtained results were evaluated according to laterally inhomogeneous barrier height analysis and effect of formation of the interfacial native oxide and the organic Pyrene thin layer between the semiconductor and top contact metal. Our aim is to study the suitability and possibility of organic/inorganic semiconductor diodes for use in barrier modification of Si metal-semiconductor diodes. For this purpose, we will investigate some junction parameters of the structure by the electrical measurements such as current-voltage and capacitance-voltage.

2. Experimental Details

Pyrene ($C_{16}H_{10}$) (99% pure) purchased from Aldrich Chemical Co. The organic/inorganic semiconductor diodes (total 43 diodes) were prepared by using one side polished (as received from the manufacturer) *n*-type Si wafer with (100) orientation and 1-10 Ω.cm resistivity, and (5.03 ± 2.4) x10^{14} cm^{-3} doping density obtained from *C-V* measurements in this study. The wafer was chemically cleaned using the RCA cleaning procedure (i.e. a 10 min boil in NH_3+H_2O_2+6H_2O followed by a 10 min boil in HCl+H_2O_2+6H_2O). The native oxide on the front surface of the substrates was removed in HF:H_2O (1:10) solution and finally was rinsed in de-ionized water for

30 s. Then, low resistivity ohmic back contact was made by evaporating Au onto the back of the n-Si substrate, then it was annealed at 420°C for 3 min in N_2 atmosphere. The native oxide on the front surface of substrate was removed in HF+10H_2O solution. Finally it was rinsed in de-ionised water for 30 s and was dried in N_2 atmosphere before forming an organic layer on the *n*-type Si substrate. Pyrene organic film was formed by thermal evaporation of Pyrene material onto the front surface of the *n*-Si wafer. To perform the electrical measurements Au top contact metal was evaporated on the Pyrene layer at 10^{-5} torr (diode area A = 0.018 cm^2).

The *I*-*V*, *C*-V and conductance(G)-voltage(V) measurements of the Au/Pyrene/*n*-Si structure were performed with KEITLEY 4200 SCS (Semiconductor Characterization System) at room temperature (see Fig. 2). Photoelectric effect on the Au/Pyrene/*n*-Si device was measured by using Scientech SF300B solar simulator.

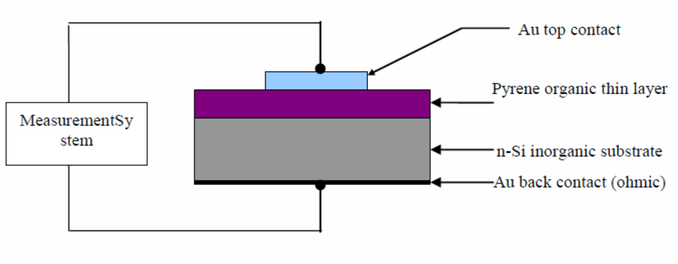

Fig. 2. The components of the Au/Pyrene/n-Si organic/inorganic semiconductor device for the electrical characterization

3. Results and Discussion

a) In-depth analysis of the dark I-V and C-V Characteristics of Au/Pyrene/n-Si MIS Diodes

The current *vs.* voltage for a Schottky barrier diode for $qV>3kT$ is given by the following well known equation named the Richardson equation [40,41].

$$I = I_0 \exp\left(\frac{qV}{nkT}\right) \tag{1}$$

Here, V is the voltage drop across the Schottky barrier, n is the ideality factor and I_0 is the saturation current determined by

$$I_0 = AA^*T^2 \exp\left(-\frac{q\Phi_b}{kT}\right) \tag{2}$$

where A is the diode area, A^* is the effective Richardson constant, k is the Boltzmann constant, T is the absolute temperature, q is the electron charge and Φ_b is the barrier height. From Eqs.1 and 2, ideality factor n and barrier height Φ_b can be written as:

$$n = \frac{q}{kT}\left(\frac{dV}{d\ln I}\right) \tag{3}$$

and

$$\Phi_b = \frac{kT}{q}\ln\left(\frac{AA^*T^2}{I_0}\right), \tag{4}$$

respectively [40,41].

Fig. 3 shows the experimental semi-log I-V characteristics of selected seven Au/Pyrene/*n*-Si MIS Schottky devices at room temperature. As clearly seen from Fig. 3, it is so good the rectifying properties of Au/Pyrene/*n*-Si MIS Schottky devices. Because, reverse bias current saturates with the applied reverse bias voltage. We formed Au/Pyrene/*n*-Si (total 43 diodes) MIS Schottky devices on the same *n*-type Si semiconductor substrate. The ideality factor *n* and BH Φ_b are obtained from the slope and the current axis intercept of the linear regions of the forward bias *I-V* plots, respectively. As seen from the Fig. 3, there is a great linear region on a logarithmic scale, in contrast to higher currents that show a curvature due to a series resistance for the MIS photovoltaic device. The values of barrier height, ideality factor and saturation current of the Au/Pyrene/*n*-Si diodes range from 0.76 eV to 0.80 eV, 1.27 to 1.64 and 5.70×10^{-9} A to 2.80×10^{-8} A, respectively. The ideality factor determined by the image-force effect alone should be close to 1.01 or 1.02 in ref. 1. Our data clearly indicate that the diodes have ideality factors that are significantly larger than this value. Higher ideality factors are attributed to secondary mechanisms which include interface dipoles due to interface doping or specific interface structure as well as fabrication-induced defects at the interface [1,5,17]. According to Tung et al. [5,8-10], the high values of *n* can also be attributed to the presence of a wide distribution of low-Schottky barrier patches caused by laterally barrier inhomogeneity.

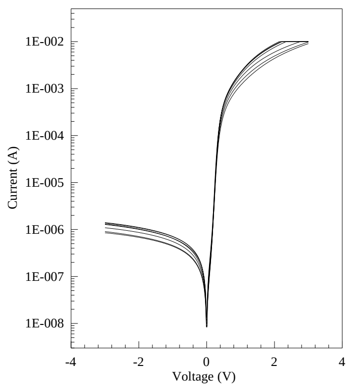

Fig. 3. Current-Voltage characteristics of the selected seven Au/Pyrene/n-Si organic/inorganic semiconductor devices

As seen from data, the effective BHs and ideality factors obtained from I-V measurements varied from diode to diode even if they are identically prepared. This result shows that the potential barrier at real organic/inorganic (OI) semiconductor interfaces depend more strongly on the applied voltage than predicted by the image-force effect for ideal contacts [1,2,38]. Therefore, it is common practice to take averages for these values. Figs. 4,5 and 6 show the statistical distributions of the BHs, the ideality factors and the saturation currents obtained from the forward I-V plots for the Au/Pyrene/*n*-Si diodes (total 43 diodes). The experimental distribution of the BHs and ideality factors were fitted by the Gaussian function. The statistical analysis of these parameters has given a mean BH value of 0.79 eV with a standard deviation of 0.01 eV, and a mean ideality factor of 1.40 with a standard deviation of 0.08 for the Au/Pyrene/*n*-Si Schottky structures. This mean BH value is much higher than 0.50 eV obtained for Au/n-Si MS structures [40]. Additionally, lateral homogeneous barrier height was calculated as 0.84 eV by extrapolation of barrier height *vs.* ideality factor curve given in Fig. 7. The value of the mean barrier height closes to lateral homogeneous barrier height as above mentioned. The case may be explained by being inhomogeneous of the Pyrene organic film/Si inorganic semiconductor interface. These findings also indicate the Pyrene organic thin film formed on inorganic substrate that the barrier height of MS Schottky diodes enhanced in significant rate. Therefore, the Pyrene organic thin films can be used for obtaining Schottky structures with higher BH in future. Recently, Van Meirhaeghe et al. [42] have found that Ag/n-GaAs and Au/n-GaAs Schottky diodes with an interfacial oxide layer (20–200 Å) showed Mott–Schottky behavior, in contrast to the usual MOS (Metal/Oxide/Semiconductor) devices. According to them [42], when a metal is evaporated on the oxidized semiconductor surface, the metal and semiconductor do not make intimate contact because of interfacial layer. Also, carrier tunneling traps localized in the interfacial layer close to the n-GaAs surface can cause Φ_b to increase [42].

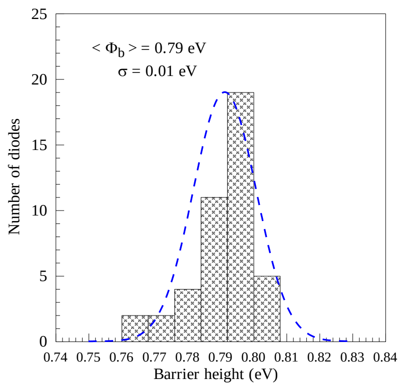

Fig. 4. The Gaussian distribution of barrier heights from the forward bias I-V characteristics of the Au/Pyrene/n-Si organic/inorganic semiconductor device.

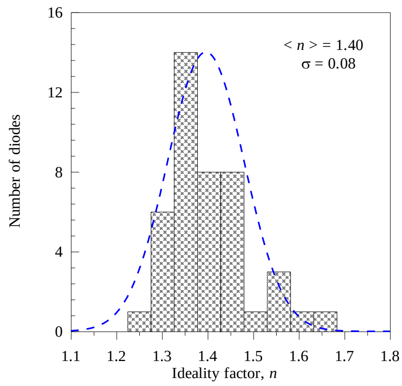

Fig. 5. The Gaussian distribution of ideality factors from the forward bias I-V characteristics of the Au/Pyrene/n-Si organic/inorganic semiconductor device

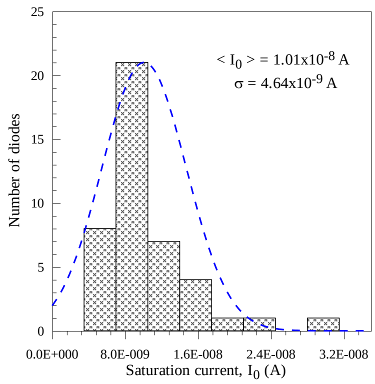

Fig. 6. The Gaussian distribution of saturation currents from the forward bias I-V characteristics of the Au/Pyrene/n-Si organic/inorganic semiconductor device

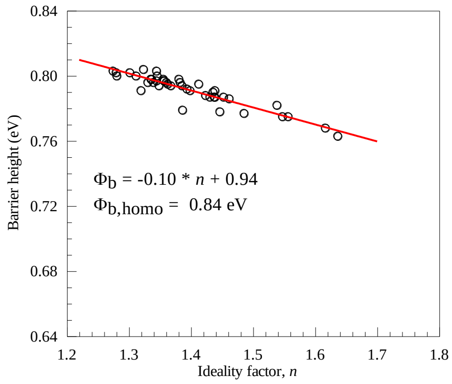

Fig. 7. The Barrier height vs. ideality factor plot obtained from the forward bias I-V characteristics of the Au/Pyrene/n-Si organic/inorganic semiconductor device

Norde proposed an alternative method to determine value of the barrier height and the series resistance (R_s) [43]. The following function has been defined in the modified Norde's method:

$$F(V) = \frac{V}{\gamma} - \frac{kT}{q} \ln\left(\frac{I(V)}{AA^{*}T^{2}}\right) \tag{5}$$

where γ is a integer (dimensionless) greater than *n*. *I*(*V*) is current obtained from the *I*–*V* curve. Once the minimum of the *F* vs. *V* plot is determined, the value of barrier height can be obtained from Eq. (6), where $F(V_0)$ is the minimum point of *F*(*V*) and V_0 is the corresponding voltage.

$$\Phi_b = F(V_0) + \frac{V_0}{\gamma} - \frac{kT}{q} \tag{6}$$

Fig. 8 shows the *F(V)*–*V* plots of the selected seven Au/Pyrene/*n*-Si diodes. From Norde's functions, R_S value can be determined as:

$$R_s = \frac{kT(\gamma - n)}{qI} \tag{7}$$

The values of Φ_b and R_s of the Au/Pyrene/*n*-Si structures have been calculated by using F(V_0) and V_0 values from the *F–V* plots. The values of barrier height and series resistance (R_s) for the Au/Pyrene/*n*-Si diodes range from 0.84 eV to 0.87 eV and 98 ohm to 327 ohm, respectively. Figs. 9 and 10 show the statistical distributions of the BHs and the series resistances obtained from the F(V)-V plots for the Au/Pyrene/*n*-Si diodes (total 43 diodes). The experimental distribution of the BHs and the series resistances were fitted by the Gaussian function. The statistical analysis of these parameters has given a mean BH value of 0.860 eV with a standard deviation of 0.006 eV, and a mean series resistance value of 226 ohm with a standard deviation of 48.7 ohm for the Au/Pyrene/*n*-Si Schottky structures. There is a good agreement the values of Φ_b obtained from the forward bias ln*I*-*V* and Norde functions. Also, the value of series resistance may be high for the higher ideality factor values. This indicates that the series resistance is a current-limiting factor for this structure. The effect of the series resistance is usually modeled with series combination of a diode and a resistance R_s. The voltage drop across a diode is expressed in terms of the total voltage drop across the diode and the resistance R_s. The high series resistance behavior may be ascribed to decrease of the exponentially increasing rate in current due to space-charge injection into the Pyrene thin film at higher forward bias voltage [44].

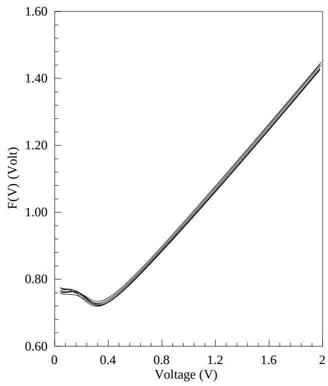

Fig. 8. Norde F(V)-V characteristics of the selected seven Au/Pyrene/n-Si organic/inorganic semiconductor devices

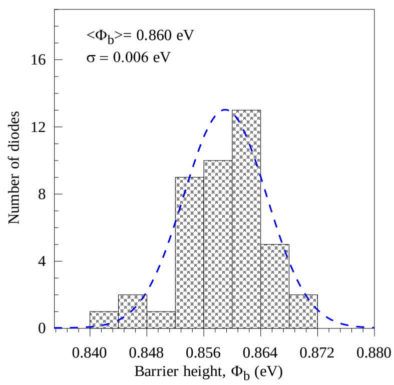

Fig. 9. The Gaussian distribution of the barrier heights from the Norde functions (F-V) of the Au/Pyrene/n-Si organic/inorganic semiconductor device

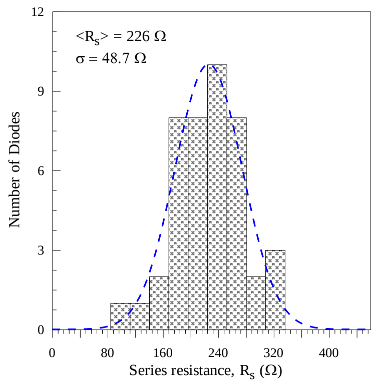

Fig. 10. The Gaussian distribution of the series resistances from the Norde functions (F-V) of the Au/Pyrene/n-Si organic/inorganic semiconductor device

The capacitance-voltage measurement is one of the most popular electrical measurement techniques used to characterize a Schottky diode. Generally, the capacitance measured in the Schottky diode depends on the reverse bias voltage and frequency. Its voltage and frequency dependence originates from the particular features of the Schottky barrier, impurity level, series resistance, interface states and interface layer between the organic layer and *n*-Si substrate, etc. At low frequency the measured capacitance is dominated by the depletion capacitance of the Schottky diode, which is bias-dependent and frequency-independent. As the frequency is increased, the total diode capacitance is affected not only by the depletion capacitance, but also the bulk resistance and dispersion capacitance, which is frequency-dependent and associated with electron emission from slowly responding deep impurity levels. Due to these effects, the bias dependent diode capacitance becomes less pronounced or disappears [45].

In Schottky structures, the depletion layer capacitance can be written as [40,41]

$$\frac{1}{C^2} = \frac{2(V_d + V)}{q\varepsilon_s A^2 N_d} \tag{8}$$

where ε_s is the dielectric constant of *n*-Si, V_d is the diffusion potential at zero bias and is determined from the extrapolation of the linear C^{-2}-V plot to the V axis. The value of the barrier height can be calculated by the relation:

$$\Phi_b(C - V) = V_d + V_n \tag{9}$$

where V_n is the potential difference between the Fermi level and the bottom of the conduction band of *n*-Si and can be calculated by knowing the donor concentration N_d and it is obtained from the following relation:

$$V_n = \frac{kT}{q}\ln\left(\frac{N_C}{N_d}\right) \tag{10}$$

where N_C =2.8x10^{19} is the density of effective states in the conduction band of n-Si [46].

Fig. 11 depicts the reverse bias *C*-V characteristics of selected seven Au/Pyrene/n-Si devices at 100 kHz at room temperature. Fig. 12 shows the C^{-2}-V characteristics of selected seven Au/Pyrene/n-Si diodes shown in Fig. 11. The barrier height, diffusion potential and donor carrier concentration values for each diode were extracted from its individual C^{-2}-V characteristics. The barrier heights, diffusion potential and acceptor carrier concentrations for the MIS devices ranged from 0.94 eV to 1.48 eV, from 0.66 V to 1.16 V and from 1.00×10^{14} cm^{-3} to 8.44×10^{14} cm^{-3}, respectively. As seen from Figs. 13,14 and 15, the experimental distributions of the barrier height, diffusion potential and donor doping concentration were fitted by the Gaussian function. The statistical analysis of the barrier heights, the diffusion potentials and donor doping concentrations obtained from C^{-2}-V characteristics has yielded a mean BH value of 1.12 eV with a standard deviation of 0.15 eV, a mean diffusion potential value of 0.84 eV with a standard deviation of 0.13 eV and a mean donor density value of 5.03×10^{14} cm^{-3} with a standard deviation of 2.4×10^{14} cm^{-3} for the Au/Pyrene/n-Si MIS devices.

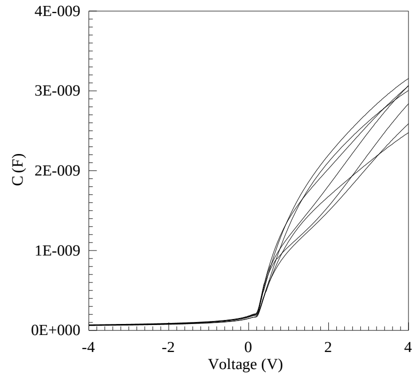

Fig. 11. Capacitance-Voltage characteristics of the selected seven Au/Pyrene/n-Si organic/inorganic semiconductor devices

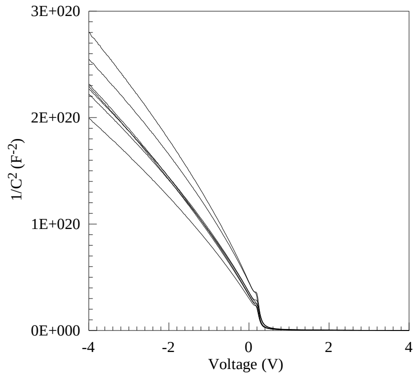

Fig. 12. 1/C^2-V plots of the selected seven Au/Pyrene/n-Si organic/inorganic semiconductor devices

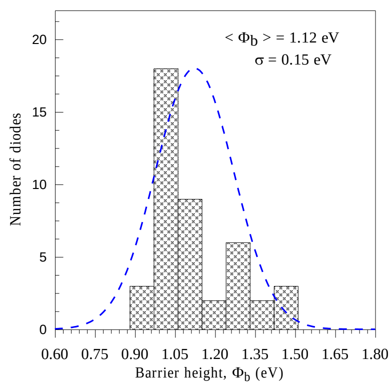

Fig. 13. The Gaussian distribution of barrier heights from the reverse bias C^{-2}-V characteristics of the Au/Pyrene/n-Si organic/inorganic semiconductor device

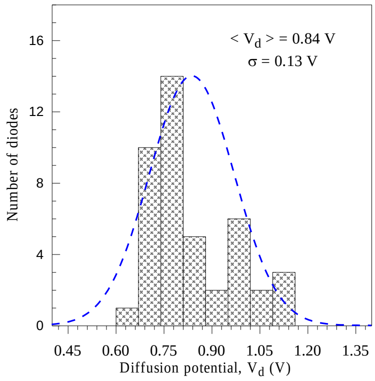

Fig. 14. The Gaussian distribution of the diffusion potential from the reverse bias C^{-2}-V characteristics of the Au/Pyrene/n-Si organic/inorganic semiconductor device

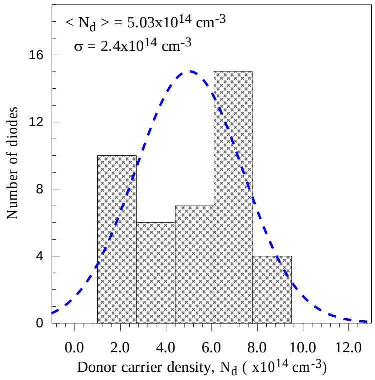

Fig. 15. The Gaussian distribution of the donor carrier concentrations from the reverse bias C^{-2}-V characteristics of the Au/Pyrene/n-Si organic/inorganic semiconductor device

According to the inhomogeneous barrier model for MS or MIS diodes, standard deviation is a measure of homogeneity of interface. In this theory, barrier height value for charge carriers at current-voltage measurements is generally lower than that of charge carriers at capacitance-voltage measurements. Due to different nature of the *C-V* and *I-V* measurement techniques, the barrier heights extracted from them are not always the same. The capacitance *C* is insensitive to potential fluctuations on a length scale of less than the space charge region and *C-V* method averages over the whole area and measures to describe BH ($\Phi_b(C-V)$ is a mean value of the barrier height distribution). The DC current *I* across the interface depends exponentially on barrier height and thus sensitively on the detailed distribution at the interface ($\Phi_b(I-V)$ is a minimum value of the barrier height distribution) [7,40]. Additionally, the discrepancy between the barrier height values of the devices may also be explained by the existence of an organic interfacial layer and trap states in semiconductor [47]. Furthermore, potential fluctuations for C-V are much higher than those for I-V. Therefore, standart deviation value (0.01 eV) for I-V is lower than that (0.15 eV) for C-V.

b) Photovoltaic and Photocapacitance Characteristics of Au/Pyrene/n-Si MIS Diodes

Fig. 16 shows the current-voltage characteristics of one Au/Pyrene/*n*-Si Schottky junction measured in dark and under 100 mW/cm^2 light illumination. As clearly seen, the device has a photosensitive behavior. Therefore, the photovoltaic parameters of the device (V_{oc} =80mV the open circuit voltage, I_{sc} = 30μA short circuit current) are obtained. Because of the presence of photovoltaic properties, Au/Pyrene/*n*-Si MIS diodes could be used as a photodiode. If the photovoltaic parameters could be made even better, the diode could be a good candidate for solar cell technology.

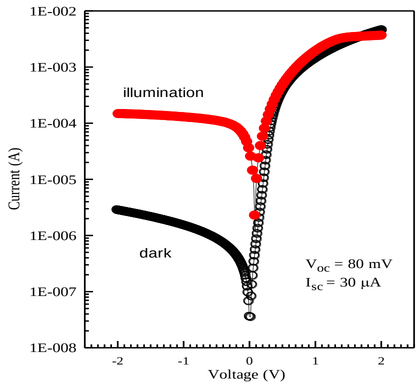

Fig. 16. (Color online) Current-Voltage characteristics of one of the Au/Pyrene/n-Si organic/inorganic semiconductor devices in dark and under light illumination.

The capacitance–voltage and conductance-voltage characteristics of one Au/Pyrene/n-Si diode in dark(black plots) and under 100 mW/cm^2 light illumination condition (red plots) at 5,10,20,30,40,50,60,70,80,90 and 100 kHz frequencies are shown in Figs.17 and 18, respectively. The light illumination increases strongly the capacitance and conductance of the device due to electron–hole charge pair generation. The capacitance and the conductance values for Au/Pyrene/*n*-Si diode under illumination are higher than those of under dark. This indicates that the light illumination increases the production of electron–hole charge pairs. The increase in charge production is dependent on the difference in the electron affinities between n-Si and pyrene layer [48].

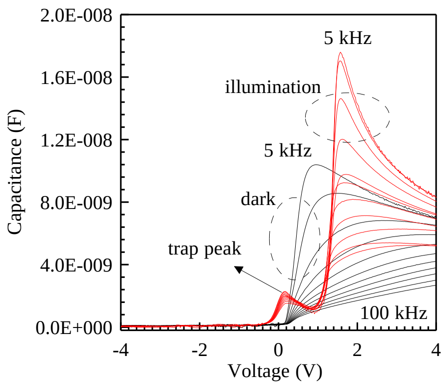

Fig. 17. (Color online) Capacitance-Voltage characteristics of the one of the Au/Pyrene/n-Si organic/inorganic semiconductor devices for various frequencies in dark and under light illumination. (Black lines are in dark, red lines are under light illumination)

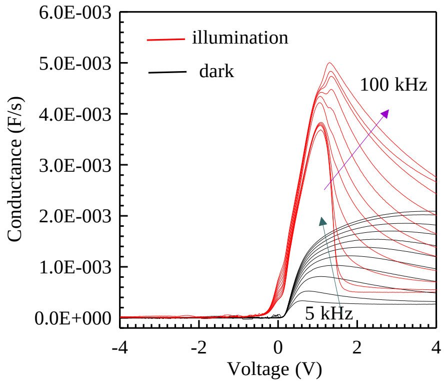

Fig. 18. (Color online) Conductance-Voltage characteristics of the one of the Au/Pyrene/n-Si organic/inorganic semiconductor devices for various frequencies in dark and under light illumination. (Black lines are in dark, red lines are under light illumination)

Furthermore, as seen in Fig. 17, the C-V characteristics show a non-monotonic dependence of capacitance on frequency giving rise to a peak at around -0.1 V for illuminated device. As the frequency increases, the magnitude of the peak decreases under the illumination effect and the position of the peak shifts slightly to the high forward bias region. This is attributed to the existence of electrically active traps [49]. Due to disordered nature of organic semiconductors, the energetic distribution of deep traps is Gaussian [50]. The presence of peak in C-V can be explained by trapping or detrapping with respect to Fermi level measured with respect to conduction band level of Si semiconductor [51].

Similarly, as seen in Fig. 18, the G-V characteristics show a non-monotonic dependence of capacitance on frequency giving rise to a peak at around 1.06 V for illuminated device. As the frequency increases, the magnitude of the peak increases under the illumination effect and the position of the peak shifts slightly to the high forward bias region. This is attributed to the existence of electrically active traps [49].

4. Conclusions

We have studied the electrical characteristics such as *I-V* and *C-V* measurements of identically prepared the Au/Pyrene/n-Si Schottky contacts formed by evaporation of organic film on *n*-Si substrate. It was seen that the pyrene organic thin film on the *n*-Si substrate showed a good rectifying behavior. The obtained results were evaluated according to laterally inhomogeneous barrier height analysis and effect of formation of the interfacial native oxide and the organic Pyrene thin layer between the semiconductor and top contact metal. It was investigated the suitability and possibility of organic/inorganic semiconductor diodes for use in barrier modification of Si metal-semiconductor diodes. Also, the photoelectric(I-V) and photocapacitance (C-V and G-V) characteristics of the Au/Pyrene/n-Si device under 100 mW/cm^2 light illumination were investigated. The open circuit voltage and short circuit current of the Au/Pyrene/n-Si device were calculated as 80 mV and 30 μA, respectively.

References

[1] R.F. Schmitsdorf, T.U. Kampen, W. Monch. J. Vac. Sci. Technol. B **15**(4), 1221 (1997).
[2] W. Monch, J. Vac. Sci. Technol. B **17**(4), 1867 (1999).
[3] Mott N F. Proc Cambridge Philos Soc **34**, 568 (1938).
[4] Bardeen J. Phys Rev 71, 717 (1947).
[5] R.T. Tung, Phys. Rev. B **45**(23), 13509 (1992).

[6] Y.P. Song, R.L. Van Meirhaeghe, W.H.Laflere, F. Cardon Solid-State Electron. **29**(6), 633 (1986).
[7] J. H. Werner and H. H. Guttler, J. Appl. Phys. **69**, 1522 (1991).
[8] J P Sullivan, R T Tung, Pinto M R, et al. J ApplPhys **70**, 7403 (1991).
[9] R T. Tung, Mater Sci Eng R, **35**(1), 83 (2001).
[10] R T. Tung, In: Brilson L J, ed. Contacts to semiconductors. New Jersey: Noyes Publishers, 1993
[11] Biber M, Cakar M, Turut A. J Mater Sci Mater Electron, **12**, 575 (2001).
[12] U. Rau, H. H. Guttler, J. H. Werner, Mater. Res. Soc. Symp. Proc. **260,** 245 (1992).
[13] J Osvald and E Dobrocka, Semicond. Sci. Technol. 11 (1996) 1198.
[14] W.P.Leroy, K.Opsomer, S.Forment, R.L.VanMeirhaeghe, Solid-State Electron. **49,** 878 (2005).
[15] M. Biber, O. Gullu, S. Forment, R.L. Van Meirhaeghe, A. Turut, Semicond.Sci. Technol. **21**, 1 (2006).
[16] C. Detavernier, R.L.VanMeirhaeghe, R.Donaton, K.Maex, F.Cardon, J.Appl.Phys. **84**(6), 3226 (1998).
[17] G.M. Vanalme, L. Goubert, R.L. Van Meirhaeghe, F. Cardon, P. Van Daele. Semicond.Sci. Technol **14**, 871 (1999).
[18] H.J. Im, Y. Ding, J.P. Pelz, W.J. Choyke, Phys. Rev. B **64**(7), 075310 (2001).
[19] M. A. Yeganeh and S. H. Rahmatollahpur, Journal of Semiconductors **31,** 074001 (2010).
[20] A. Turut, F. Koleli, J. Appl. Phys. **72**(2), 818 (1992).
[21] Y. Onganer, M.Saglam, A.Turut, H.Efeoglu, S.Tuzemen, Solid-State Electron. **39**, 677 (1996).
[22] P.S. Abthagir, R. Saraswathi, Organic Electronics **5**(6), 299 (2004).
[23] L.M. Huang, T.C. Wen, A. Gopalan, Thin Solid Films **473**(2), 300 (2005).
[24] K. Kaneto, J. Nakajima, M. Nakagawa, W. Takashima, Thin Solid Films **438**, 195 (2003).
[25] S. Aydogan, M. Saglam, A. Turut, Vacuum **77**(3), 269 (2005).
[26] M. Cakar, A. Turut, Synthetic Met. **138**, 549 (2003).
[27] T. Kampen, A. Schuller, D.R.T. Zahn, B. Biel, J. Ortega, R. Perez, F. Flores, Appl. Surf. Sci. **234**(1–4), 341 (2004).
[28] A.R.V. Roberts, D.A. Evans, Appl. Phys. Lett. **86**, 072105 (2005).
[29] A. Bolognesi, A. Di Carlo, P. Lugli, T. Kampen, D.R.T. Zahn, J. Phys.: Condens. Matter **15**, S2719 (2003).
[30] M. Cakar, C.Temirci, A. Turut Synthetic Metals **142**(1-3), 177 (2004).
[31] F.Yakuphanoglu, Physica B **389**, 306 (2007).
[32] O. Gullu, A. Turut and S. Asubay, J. Phys.: Condens. Matter **20**(4), 045215 (2008).
[33] S.K. Park, C. Lee, K.C. Min, N.S. Lee, Bull. Korean Chem. Soc. **25**(12), 1817 (2004).
[34] M. Sakomura, T. Nakashima, K. Ueda, M. Fujihira, Colloids Surfaces A: Physicochemical and Engineering Aspects **284/285**, 528 (2006)
[35] D. Bhattacharjee, K. Mukherjee, T. N. Misra, J Phys. Chem. Solids **61** (5) 751 (2000)
[36] Y. Takahashi, T. Kitamura, K. Uchida, Journal of Luminescence, **27**(4), 449 (1982-1983).
[37] B. J. Basu, A. Thirumurugan, A.R. Dinesh, C. Anandan, K.S. Rajam, Sensors and Actuators B **104**, 15 (2005).
[38] H. Cetin, B. Sahin, E. Ayyildiz, A. Turut, Physica B **364**, 133 (2005).
[39] S. Altindal, H. Kanbur, A. Tataroglu, M.M. Bülbül, Physica B **399**, 146 (2007).
[40] E.H. Rhoderick, R.H. Williams, Metal–Semiconductor Contacts, 2nd ed. Clarendon, Oxford, 1988.
[41] S.M. Sze, Physics of Semiconductor Devices, 2nd ed. Wiley, New York, 1981.
[42] R.L. Van Meirhaeghe, W.H. Laflere, F. Cardon, Solid-State Electron. 16 (1983) 1189.
[43] S. Karatas, S. Altindal, A. Turut and M. Cakar, Physica B **392**(1-2), 43 (2007).
[44] S Aydogan, Ö Güllü and A Türüt, Phys. Scr. **79,** 035802 (2009).
[45] E H Nicollian, A Goetzberger, Bell Syst. Tech. J. **46** 1055 (1967).
[46] D.A. Neamen, Semiconductors Physics and Devices, R. R. Donnelley & Sons Company, Sydney, 1992.
[47] H.C. Card, E.H. Rhoderick, J. Phys. D **4**, 1589 (1971).

[48] K Akkılıç, F. Yakuphanoglu Microelectronic Eng. **85**, 1826 (2008).
[49] MJ Lee, S Seo, DC Kim, SE Ahn, DH Seo, IK Yoo, IG Baek, DS Kim, IS Byun, SH Kim, IR Hwang, JS Kim, SH Jeon, BH Park, Adv Mater 19, 73 (2007).
[50] J Steiger, R Schmechel, H.von Seggern Synth Met 129, 1 (2002).
[51] A Sharma, P Kumar, B Singh, SR Chaudhuri, S. Ghosh Appl Phys Lett **99**, 023301 (2011).